Influence of Phosphate on Bacterial Adhesion onto Iron Oxyhydroxide in Drinking Water

ARTICLE *in* ENVIRONMENTAL SCIENCE AND TECHNOLOGY · MARCH 2002

Impact Factor: 5.33 · DOI: 10.1021/es010155m · Source: PubMed

4 AUTHORS, INCLUDING:

Brice M R Appenzeller
LIH Luxembourg Institute of Health
56 PUBLICATIONS **737** CITATIONS

SEE PROFILE

Environ. Sci. Technol. **2002**, *36,* 646−652

Influence of Phosphate on Bacterial Adhesion onto Iron Oxyhydroxide in Drinking Water

BRICE M. R. APPENZELLER,[†,‡] YANN B. DUVAL,[‡] FABIEN THOMAS,[‡] AND JEAN-CLAUDE BLOCK*[,†]

LCPME, CNRS-UHP, Faculté de Pharmacie, Pôle de l'eau, 15 avenue du Charmois, F 54500 Vandoeuvre, France, and LEM-GRESD, CNRS-INPL, BP 40, F 54500 Vandoeuvre, France

The transport and storage of drinking water in water distribution systems can modify its initial composition and properties. The accumulation of bacteria on corroded pipes is prejudicial and may lower the microbiological quality of the water. Previous results have shown that when pipes are highly corroded, the addition of phosphate, used as an anticorrosion treatment, decreases the bacterial concentration in the water. We studied the possibility of using phosphate to reverse the surface charge of iron oxyhydroxide (FeOOH) to limit bacterial adhesion. Iron oxyhydroxide (IOH) particles and *Escherichia coli* SH 702 were used as models of corrosion products and bacterial contamination, respectively. Electrophoresis was used to characterize the initial surface charges of both types of particles and the modifications that occurred after the addition of phosphate anions. Flow cytometry and adhesion assays were used to build adsorption isotherms of bacteria on IOH versus (phosphated-) IOH. X-ray photoelectron spectroscopy permitted to determine the chemical composition of the *E. coli* envelope and to discuss on functional groups responsible for bacterial surface properties. In the present conditions, adding phosphate to water allowed a decrease of 75% of the bacteria adhering to IOH.

Introduction

Although bacterial growth associated with the presence of iron is not harmful in soils, it becomes particularly worrying when it occurs in drinking water distribution systems. Large accumulations of bacterial cells are actually reported to be colocated with ferric minerals in the environment or with corrosion products of metallic infrastructures (*1, 2*). This affinity of bacteria for rust may be linked to several phenomena, such as the high surface area of the oxides particles available for bacterial adsorption (*3*), the role of these oxides as potential electron acceptors, which may increase bacterial activity (*4*), or their ability to adsorb large amounts of organic matter (*5*) which may be subsequently biodegraded by microorganisms.

In water distribution systems, the interaction between bacteria and iron species, such as corrosion products of pipes or deposits (*6*), can deteriorate the microbiological quality of drinking water because it increases the bacterial concentration in the biofilm fixed on pipe walls and in the bulk water (*7*−*10*). Moreover, bacteria attached to surfaces or to particles are shown to be much more difficult to inactivate by disinfectants (*11, 12*).

Phosphate treatments are usually applied to large drinking water networks to control corrosion and the release of metals into the water. This procedure is highly controversial. One disadvantage of this procedure is that phosphate may serve as a nutrient for the microorganisms, which will sustain bacterial growth in waters with limited amounts of phosphate (*13, 14*). However, the addition of phosphate to drinking water networks has been shown to increase the water quality by reducing biofilms, improving the efficiency of disinfectants, decreasing the occurrence of coliforms, and surprisingly by drastically reducing bacterial production (*7, 10, 15*). These observations suggest that the favorable environment provided by the corrosion products is probably modified by the phosphate, making the environment less suitable for bacterial development. Among the various factors that might produce such an effect, we investigated the initial attachment process, which is assumed to be a determining step in the colonization of the surface by microorganisms (*16*). Although the process of bacterial adhesion to surfaces is governed by several parameters such as hydrophobic interactions, van der Waals forces and electrostatic interactions (*17*−*19*), we focused on the ability of phosphate anions to reverse the surface charge of iron oxyhydroxides from positive to negative (*20*), which would consequently limit the sorption of negatively charged bacterial cells. Previous studies showed that the attachment of bacteria to solid substrates (e.g. metals) can be inhibited by making surfaces negatively charged with adsorbed molecules (*21*). Long-range repulsive forces probably play a major role in preventing bacterial attachment. This observation provides further information on the consequences of adding phosphate to drinking water distribution systems.

In this study, IOH (iron oxyhydroxide = FeOOH) particles and *Escherichia coli* were used as models of corrosion byproducts and bacterial contamination, respectively. The ability of phosphate anions to reverse the charge of IOH particles and the resultant effects on cell attachment were studied. The surface charge of the bacteria and the IOH particles was estimated by measuring their electrophoretic mobility. X-ray photoelectron spectroscopy (XPS) was used to determine the elemental composition and major chemical groups of the outer surface (around 10 atomic layers) of the bacterial envelope. The adhesion of *E. coli* to phosphated and nonphosphated IOH particles was quantified, and the comparison of adsorption isotherms was allowed to propose that the addition of phosphate to water can limit bacterial adhesion to iron oxide.

Experimental Section

Iron Oxyhydroxide Particles. IOH was synthesized by gently adding 1 M NaOH to 500 mL of 1 M $FeCl_3$ solution until the solution reached pH 10, at 25 °C, with magnetic stirring. The precipitate was then washed three times with ultrapure water by settling and removal of the supernatant. It was then harvested on filter and left to air-dry for 3 days at 25 °C. The resultant solid was crushed with a pestle and mortar and sieved to keep the fraction between 150 and 38 μm. The mean and median values of size distribution, measured by laser diffraction, were close to 100 μm (Table 1). The prepared powder displayed the characteristic X-ray diffraction pattern of goethite (α-FeOOH) (Figure 1) and contained at least 25% amorphous oxyhydroxide. The BET specific surface area,

* Corresponding author phone: +33 (0) 383 59 62 56; fax: +33 (0) 383 59 62 60; e-mail: Jean-Claude.Block@pharma.uhp-nancy.fr.
† LCPME, CNRS-UHP.
‡ LEM-GRESD, CNRS-INPL.

10.1021/es010155m CCC: $22.00
Published on Web 01/15/2002

TABLE 1. Physicochemical Characteristics of Particles in Mineral Water

particle	iep (pH)	zeta potential at pH = 7 (mV)	size distribution median (μm)	size distribution mean (μm)	octane adhesion (% abs)
E. coli SH702	≈1	−18 ± 2.3	1.05	1.6 ± 1.7	18.5 ± 1.9
IOH	8.9 ± 0.2	10 ± 2.5	100.8	103.3 ± 62.3	14.1 ± 3.4
phosphated IOH	4.3 ± 0.1	−5.3 ± 2.5	99.5	104.0 ± 64.5	0.1 ± 0.5

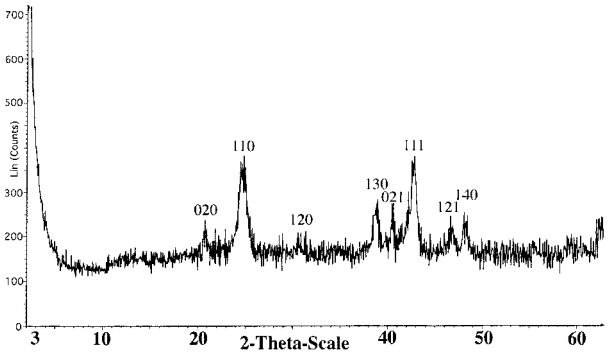

FIGURE 1. X-ray diffraction spectra of IOH with typical Miller indices of goethite (α-FeOOH).

TABLE 2. XPS Analysis of the Chemical Composition of *E. coli* Envelope[a]

element			
C	O	N	P
63.2[b]	31.4[b]	4.9[b]	0.4[b]

ratio of charged functional groups in the cell envelope		
carboxyl/amine	carboxyl/phosphate	amine/phosphate
4.5	13.5	3

[a] Percentage of carboxyl group was determined from C1s, amine from C1s and N1s, and phosphate from P2p. Positions of the peaks determined by decomposition of C1s were 288.15 and 285.9 eV for carboxyl and amine, respectively. fwhm were 1.82 eV for carboxyl and 0.95 eV for amine. Position of the amine peak determined from N1s was 401.0 eV and fwhm was 2.95 eV. Position of the phosphate peak was 133.30 eV and FHWM was 2.57 eV. [b] Percentage of element in the cell envelope.

measured by N_2 gas adsorption, was 114 m^2 g^{-1}. The adsorption isotherm showed no substantial evidence for micropores (<20 Å). A so-called "phosphated IOH" was prepared as a suspension of 1 g L^{-1} IOH in mineral water containing 8 mg P L^{-1} phosphate (2.58×10^{-4} mol L^{-1}).

***Escherichia coli* Culture.** *Escherichia coli* SH 702 was used in these experiments. The physicochemical characteristics of the bacteria are listed in Table 1, and the chemical composition of the cell envelope of *E. coli* is listed in Table 2. Bacteria were grown in LB broth media (Difco 0446-17-3) at 25 °C. After 48 h, the cell cultures were washed three times by centrifugation (5 min; 10 000 g) and suspended in commercial mineral water (Evian) with a constant mineral composition (mg L^{-1}: Ca: 78; Mg: 24; Na: 5; K: 1; HCO_3: 357; SO_4: 10; Cl: 4.5; NO_3: 3.8; SiO_2: 13.5; solids at 180 °C: 309). The cells were then left to starve in the same water at 20 °C for 24 h before being submitted to another washing cycle. The cells were then harvested and diluted to a concentration of $\sim 1 \times 10^9$ cells ml^{-1}.

Bacterial Counting by Flow Cytometry. Bacteria were counted with a *FACScalibur 3CS* flow cytometer (Becton Dickinson 352054) equipped with an air-cooled laser providing 15 mW at 488 nm and the standard filter setup. Stained bacterial cells, excited at 488 nm, were enumerated according to their side scattering (SSC channel) and green fluorescence (FL1 channel) collected at 530 nm. All cell parameters were recorded on a logarithmic scale with 4 orders of magnitude mapped onto 1024 channels. Before bacterial cells were enumerated, the background noise of both water and particles were gated out with a threshold of 500 channels applied to the fluorescence signal. A window was subsequently drawn around the predicted area containing *E. coli* to exclude the remaining background. Cells were enumerated over a defined period of time (1 min) at a given flow rate, which was calibrated at the beginning and end of each analysis session. Yellow-green fluorescent microspheres (0.95 μm diameter fluorescent size-standard beads; Polyscience inc., Warrington, Pa) were systematically added to each sample as an internal reference. Samples were diluted so that between 3000 and 30 000 events occurred per minute. Subsamples (1 mL) were put into plastic tubes (12 mm × 75 mm) and directly incubated with *SYBR Green II* RNA gel stain (final concentration = 5 μM) for 10 min at room temperature in the dark.

XPS Analysis of the *E. coli* Envelope. Samples of *E. coli* were prepared for XPS analysis as described by Van der Mei et al. (*22*).

Bacteria were harvested from culture media after a 24 h-growth time. Cells were then washed by three centrifugations (10 min, 5000 g) and resuspension in ultrapure water. The deposit obtained after the last centrifugation was frozen in liquid nitrogen and then dried by low-pressure desiccation. Cells were then harvested and laid down on a copper support. It was slightly pressed to reach a regular coat and then submitted to XPS analysis. X-ray photoelectron spectra were recorded by a Leybold-Herakus spectrometer equipped with a multidetection electron energy analyzer (VSW FAT mode HA150). The nonmonochromatized radiation source (Mg-Kα, 1253.6 eV) operated at 15 kV and 10 mA. The working pressure was typically $<10^{-8}$ mbar. The measurements were recorded with a takeoff angle of ∼90°. A gold standard (Au $4f_{7/2}$ line at 83.8 eV) was used to calibrate the spectrometer, giving a binding energy reproducibilty of ±0.15 eV. First, extended spectra were collected in the range 0−1100 eV (1 eV step, 0.1 s $step^{-1}$). Subsequently, detailed spectra were recorded for the following regions: O1s, C1s, N1s, P2p (0.05 eV step, 0.1 s $step^{-1}$). The number of acquisitions was adjusted for each element to obtain a satisfactory signal-to-noise ratio. A charging effect of 2.5−3 eV was observed, and all binding energies were referenced to the C−H photopeak (C1s line at 284.6 eV). After a Shirley-type background subtraction, the raw spectra were fitted by use of a curve-fitting program with pure Gaussian peak shape. Spectra of pure chemical products (threonine, glycine, glutamic acid, and glucose) carrying the major organic groups expected at the surface of *E. coli* envelope were recorded. From these spectra were deducted reference positions of functional groups carboxyl, aliphatic, ether, alcohol, amine, and amide (residual polymerization of amino acids). The relative positions obtained (Table 2) were confirmed by literature. These reference positions were then used to decompose C1s and N1s lines of spectra obtained from *E. coli* SH 702 XPS analysis and allowed to attribute functional group to each peak. The relative abundance of each function on the bacterial cell surface was deduced from the area of its corresponding peak (Table 2). In the present experimental

conditions of circumneutral pH, carboxyl and amine functions are likely to be deprotonated and protonated, respectively. Nevertheless, the denomination carboxyl and amine were preferred than carboxylate and ammonium.

Electrokinetic Measurements. The zeta potential of bacteria and IOH particles was determined by use of a zetaphoremeter III (Sephy & CAD instrumentations) apparatus.

The measurement cell was made of a calibrated quartz channel fit between two reservoirs containing the electrodes. The channel was lit with a 2-mW He/Ne laser source to obtain the scattering spots of the particles located at the stationary layer. A 100 V electric field was alternatively applied (five times, 1 s in each direction), and the velocity of the particles was recorded by use of a microscope and a CCD camera coupled to a timed image analysis computer program. The electrokinetic potential (or ζ potential) was calculated by the Helmholtz-Smoluchowski equation

$$\zeta = \eta\mu/\epsilon E$$

where ζ is the zeta potential (mV); η is the viscosity (Pa s); μ is the velocity (μm s^{-1}); E is the electric field (V cm); and ϵ is the permittivity (F m^{-1}).

Electrokinetic measurements were taken on bacterial suspensions at concentrations of between 1.0 and 5.0 $\times$ 10^7 cells mL^{-1} and on 1 g L^{-1} goethite suspensions. The pH was adjusted with 0.1 M HCl and 0.1 M NaOH.

The measurements were carried out in media with different characteristics: commercial mineral water Evian (0.5 mS cm^{-1}), 0.1 M KCl (12 mS cm^{-1}), and 1 M KCl (120 mS cm^{-1}).

Phosphate Source and Dose. A stock solution of 3.22 $\times$ 10^{-3} mol L^{-1} NaH_2PO_4, pH 7, was used as a phosphate source for all assays. The phosphate concentration was measured according to the stannous chloride spectrophotometric method (*23*). Samples of 5 mL were diluted to 100 mL with ultrapure water, and 1 mL of glycerol/$SnCl_2$ solution and 1 mL of ammonium molybdate were added. The samples were mixed and left to stand for 10 min, and the absorbance was measured at 690 nm against a blank without phosphate (spectrophotometer ATI UNICAM-UV/visible Software V3.01). The results are expressed as mg P-PO_4 L^{-1}.

Adhesion to Octane. Assays to measure the adhesion of particles to octane were adapted from the test developed by Rosenberg et al. (*24*). The octane adhesion test was applied to bacteria and IOH particle suspensions with an absorbance at 600 nm lower than 0.3 units. Bacteria were harvested after the starvation step and the final washing cycle and suspended in mineral water to obtain the suitable concentration. Phosphated and nonphosphated IOH particles were harvested from the supernatant of 1 g L^{-1} (size $<$ 38 μm) suspensions that had been shaken for 24 h and then left to settle. In all cases, 2.5 mL of suspension (bacteria or (phosphated-)IOH) was vigorously mixed (Heidolph DSG 3/2 vibratory agitator) for 120 s with 1 mL of *n*-octane (Aldrich, 0-325-7) in a glass tube (Ø = 10 mm). After 5 min a sample of the aqueous phase was taken, and the absorbance at 600 nm was measured. The results are expressed as the following: (Ai − Af)/Ai (Ai, absorbance of the initial suspension; Af, absorbance after octane adhesion).

Bacterial Adhesion Experiments. All bacterial adhesion experiments were carried out in 120 mL-glass flasks. IOH particles (0.1 g) were conditioned in 90 mL of commercial mineral water, with or without additional phosphate. Suspensions were then shaken at 26 rev min^{-1} (Comfort Heto Master Mix) for 24 h at 20 °C, to reach the equilibrium of phosphate adsorption onto IOH. The pH was adjusted to 7 with 0.1 M HCl. Bacterial cells were added from the stock suspension in flasks to initial concentrations ranging from 4.75 $\times$ 10^6 to 6.14 $\times$ 10^8 cells mL^{-1} (final volume: 100 mL). The flasks were then shaken at 26 rev min^{-1} at 20 °C for 2 h contact time. Samples (10 mL) from flasks were then centrifuged for 1 min at 1800 rpm to remove IOH particles and any attached bacteria. Samples of the supernatant (5 mL) were collected for the enumeration of suspended, nonattached bacteria. The number of bacteria attached to IOH particles was calculated by subtracting the number of free bacteria from the initial number of bacteria.

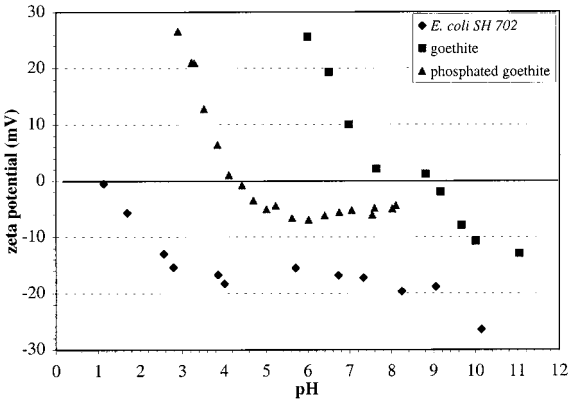

FIGURE 2. Zeta potential of *E. coli*, IOH, and 3.2 $\times$ 10^{-5} M phosphated IOH in mineral water at varying pH.

Results and Discussion

Characterization of Bacteria and Oxyhydroxide Particles. *Bacteria*. The bacteria were negatively charged in the pH range between pH 1.2 and 10 (Figure 2). The measurements were taken in mineral water with a conductivity of 0.5 mS cm^{-1}, which indicates an approximate ionic strength of 5 $\times$ 10^{-3} M. The isoelectric point (iep = pH whom zeta potential equals to zero) was approximately pH 1. The data points below pH 3 reflect a decrease in the surface charge and increased surface charge screening at high ionic strength. Such a variation in surface charge results from the successive protonation of the organic functional groups present in the surface structures forming the cell walls of microorganisms (*25*−*27*). Amino acids are always present at the surface of bacteria, and, therefore, carboxylic and amino groups are expected to be present. Previous studies using acidimetric titration showed that three proton active surface functional groups are present on bacterial cell wall: carboxyl, phosphate, and hydroxyl groups with acidity constants (pK_a) of 4.82 $\pm$ 0.14, 6.9 $\pm$ 0.5, and 9.4 $\pm$ 0.6, respectively (*25, 28*). Other studies attributed a pK_a close to 2.1 to phosphate involved in phosphodiester bridges (R−O−HPO_2−O−R/R−O−PO^-_2−O−R), in the techoic acids of Gram positive bacteria or included in polymers (R−H_2PO_4/R−HPO^-_4) as in phospholipids (*26*); a pK_a of about 2.8 was attributed to polysaccharide-associated COOH/COO. Compared to most common bacteria, the iep value of *E. coli* SH 702 was relatively low. Nevertheless, iep below 2 have also been observed in other *E. coli* strains (*29*), in *Pseudomonas*, and in coryneform bacteria (*26*). As suggested by Rijnaarts et al. (*26*), an iep$\leq$ 2.8 would indicate the presence of significant amounts of cell surface polymers containing negatively charged phosphate and/or carboxyl groups, and an iep$\leq$ 2 would only result from the presence of phosphate groups in the cell envelope (*26, 27*). According to the structure of Gram-negative bacteria like *E. coli*, phosphate groups are also incorporated in lipopolysaccharides (*30, 31*). As hydroxyl groups are still protonated at pH = 7, it is reasonable to assume that only carboxyl and phosphate groups contribute to the negative charge. Moreover, the negative charge of the overall cell wall clearly shows that amino groups are unlikely to contribute significantly to the charge of the bacterial surface even though

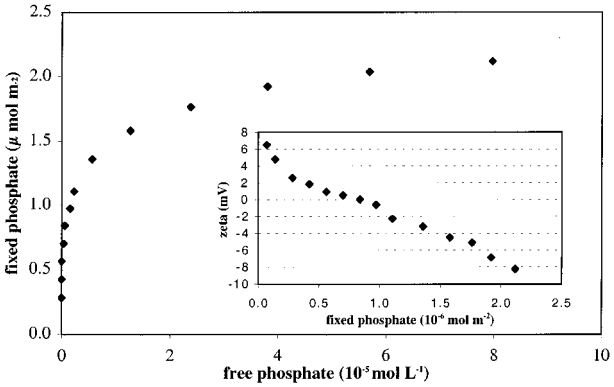

FIGURE 3. Large frame: isotherm of phosphate adsorption on IOH particles in mineral water, at pH = 7, 20 °C. Small frame: zeta potential versus fixed phosphate for IOH particles in mineral water, at pH = 7, 20 °C.

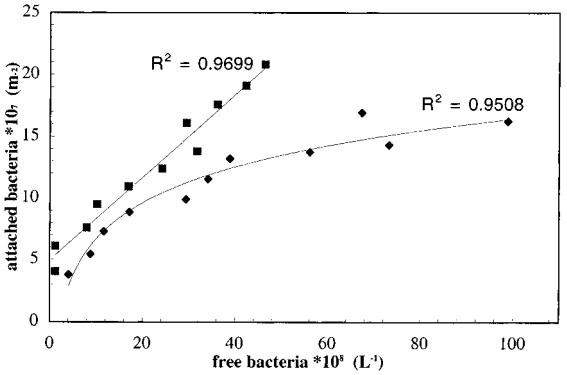

FIGURE 4. Adsorption isotherms of *E. coli* on (■) IOH and on (◆) 3.2 × 10^{-5} M phosphated IOH in mineral water at pH = 7, 20 °C, after 2 h contact time at 26 rev min^{-1} agitation.

some of them are positively charged. This observation was supported by our XPS analysis of the *E. coli* envelope (Table 2). The elemental composition reveals the presence of P, N, C, and O atoms, which correspond respectively to the following: P, phosphate groups; N, amine and amide groups; C, carboxyl, amine, amide, ether, ester, alcohol, and aliphatic groups; and O, all oxygenated groups. Decomposition of the C and N lines and comparison with reference molecules allowed us to identify and quantify the major organic groups, among which the charged groups are of interest in the present work. The abundance ratios of these groups showed that carboxyl groups are common in the structure and are the most common charged groups in the bacterial envelope.

Iron Oxyhydroxide. The IOH synthesized for these experiments was supposed to represent the external layer of the corrosion products found in pipes described as "brown-orange deposit" (*32*) or "red rust" (*6*). This is the layer that is in direct contact with the water and free bacteria. Transmission electronic microscopy analysis of these corrosion products revealed that they contained both well crystallized (goethite, α-FeOOH) and poorly crystallized iron oxyhydroxide (results not shown). X-ray diffraction analysis revealed that synthesized IOH particles were composed of goethite (α-FeOOH) and amorphous iron oxyhydroxide (Figure 1). The value of iep = 8.9 for IOH (Table 1) is consistent with previous studies, which reported values between pH = 8 and pH = 9 (*20, 33*). In the presence of 2.58 × 10^{-4} M of phosphate, the iep was shifted to pH 4.3. This shows that phosphate adsorbs to positively charged sites. Similar shifts were reported by Bowden et al. (*33*) (from 8.4 to 4.3) and by Parfitt and Atkinson (*20*) (from 8.1 to 5.1).

Adsorption of Phosphate on Iron Oxyhydroxide Particles. Phosphate was very strongly adsorbed on IOH, as shown by the vertical slope at the lowest equilibrium concentrations (Figure 3). In fact, no phosphate was measured in solution when less than 9.67 × 10^{-5} mol L^{-1} (3 mg P/L) was added (0.84 μmol m^{-2} fixed). The slope of the isotherm was very steep for equilibrium concentrations below 2 × 10^{-5} mol L^{-1}. For higher concentrations, the adsorbed quantity tends toward a plateau around 2.1 × 10^{-6} mol m^{-2}. The ability to adsorb large amounts of phosphate anions was previously observed with goethite or other iron oxyhydroxides (*20, 33*−*35*). This phenomenon resulted in very low concentrations of dissolved phosphate in the water bulk when the surface coverage of IOH was low. This affinity of IOH for phosphate is even stronger than for all other inorganic or organic anions (*34, 35*). Nevertheless, the adsorption process had to be tested in each condition, because the equilibrium depends on the size and nature of the particles used (*36*) and on the composition and ionic strength of the medium. The amount of phosphate adsorbed on oxyhydroxide (2.2 × 10^{-4} mol g^{-1} in equilibrium with 3.22 × 10^{-5} mol L^{-1} = 1 mg P L^{-1} of free phosphate) was comparable to that reported by other studies (0.34 × 10^{-4} to 1.62 × 10^{-4} mol P g^{-1}) (*33, 37*−*39*).

Another important event during phosphate adsorption on iron oxyhydroxide is the modification of the surface charge of the particles. The zeta potential decreased from around +7 mV in the absence of phosphate to below −8 mV when more than 2 × 10^{-6} mol m^{-2} were fixed (32 × 10^{-5} mol L^{-1} added) (Figure 3). It was then possible to cancel the mineral initial surface charge having a free phosphate concentration near zero (about 0.84 × 10^{-6} mol m^{-2} fixed). With 7 × 10^{-5} mol L^{-1} of phosphate in water (equal to the maximum amount of phosphate authorized in drinking water in the E.U. = 5 mg L^{-1} P_2O_5), the adsorbed anions clearly conferred a negative charge to the particles. Free phosphate in solution was only measured when more than 9.67 × 10^{-5} mol L^{-1} (3 mg P L^{-1}) was added. From this value, the surface charge of IOH particles became negative (Figure 3). The adsorption of phosphate anions was still possible, meaning that some sites were still available even though the surface charge of particles was negative. This observation shows the role of surface charge in the adsorption of phosphate anions on surface sites as described by Bowden et al. (*33*).

Bacterial Adhesion. Adhesion assays revealed that *E. coli* rapidly attached to IOH particles, and a pseudoequilibrium was reached within 2 h (data not shown). This observation is consistent with previous studies on different bacteria/sorbant systems, such as *Thiobacillus ferrooxidans* onto sulfide minerals or quartz or *E. coli* onto poly(methacrylates), and demonstrated that the adhesion of bacteria to minerals almost reached equilibrium within a few hours (*40, 41*). Other studies carried out with *Bacillus subtilis* on corundum (α-Al_2O_3) and quartz (SiO_2) indicated that the adhesion of bacteria onto a mineral surface is rapid and that equilibrium is reached in less than 1 h (*42*).

To observe the effect of phosphate on bacterial adhesion onto IOH, isotherms were built with IOH particles in mineral water, and in mineral water supplemented with 2.58 × 10^{-4} mol L^{-1} phosphate (8 mg P−PO_4 L^{-1}) (Figure 4). The adsorption isotherm of bacteria on IOH without phosphate displayed a high ability of the surface to adsorb bacterial cells. The percentage of attached bacteria varied from 98% (when 4.75 × 10^9 L^{-1} cells were added) to 84% (when 2.85 × 10^{10} L^{-1} cells were added). If each adsorbed bacterium occupies 1 μm^2, only 0.021% of the IOH surface was covered at the highest bacteria content. Although the entire surface displayed by the oxyhydroxide was probably not available for bacteria, the monotonic increase in adsorption as the cell concentration increased indicates that, in this case, the surface of the mineral was not saturated with respect to

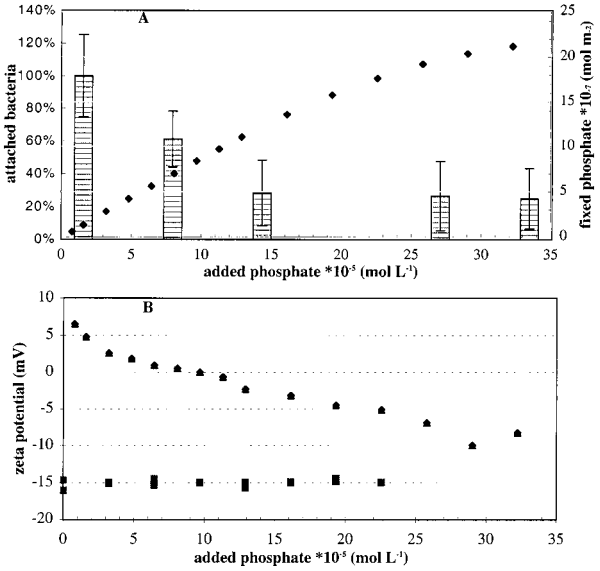

FIGURE 5. A; (blocks) attached bacteria versus added phosphate for 6.14×10^{11} L^{-1} initial added *E. coli* in mineral water at pH = 7, after 2 h contact time. Reference block of 100% (for no added phosphate) corresponds to 2.04×10^{11} cells g^{-1} of adhering bacteria. Other adhering bacteria amounts were reported to this value to assess percentage of decreasing adhesion. (◆) fixed phosphate versus added phosphate in mineral water at pH = 7 after 24 h contact time. B; zeta potential versus added phosphate in mineral water at pH = 7, after 2 h contact time for (■) *E. coli* and for (▲) IOH particles.

adsorbed bacteria. Nevertheless, it is reasonable to assume that adsorption would obviously become site-limited at higher bacteria:mineral ratios. Comparing bacterial adhesion onto IOH and onto phosphated IOH (Figure 4) showed that the effect of phosphate anions on bacterial attachment was relatively slight at low bacterial concentrations but that it became more noticeable as the number of bacteria increased. The number of bacteria attached to phosphated IOH was always inferior to the number of bacteria attached to the corresponding IOH and varied from 91% (4.75×10^9 L^{-1} total added cells) to 65% (2.85×10^{10} L^{-1} total added cells). At the latter value, it was estimated that approximately 0.016% of the mineral surface was covered by bacteria. Although bacterial adhesion is thought to increase when more bacteria are added, the nonlinear shape of the isotherm obtained with phosphated IOH particles clearly shows the onset of the surface saturation. This highlights the modification of the mineral surface due to the adsorption of phosphate anions.

To better observe the modifications resulting from the addition of phosphate to the mineral surface and the resulting changes in bacterial adhesion, assays were also conducted with constant numbers of bacteria and varying quantities of phosphate. The isotherms (Figure 4) showed that it was preferable to add a high initial bacteria concentration (6.14×10^{11} cells L^{-1}) to obtain a clearly marked effect. Bacterial adhesion was observed as phosphate was progressively added and fixed (Figure 5A). The amount of bacteria adhering (2.04×10^{11} cells g^{-1}) to IOH without phosphate was considered to be 100% so that we could evaluate the decrease in bacterial adhesion when phosphate was added. In this first case, bacteria covered about 0.18% of the mineral surface. When further phosphate was added, the amount of phosphate fixed to IOH increased and progressively reversed the surface charge of mineral particles (Figure 5B). It led to the simultaneous decrease in bacterial attachment, tending to a constant value of about 25% (5.03×10^{10} attached cells g^{-1} for 33×10^{-5} mol L^{-1} added phosphate), corresponding to 0.047% of mineral surface covered. The comparison of Figure 5 (parts A and B) shows that this constant seems to be reached when IOH particles and bacteria become charged alike. It highlights the role of electrostatic interactions, which varied from attraction (+7 mV and −15 mV for IOH and *E. coli*, respectively) to repulsion (−10 mV and −15 mV for IOH and *E. coli*, respectively) when phosphate was added (Figure 5B). The behavior of bacterial adhesion to IOH particles with respect to added phosphate observed in Figure 5A,B can be discussed according to the Derjaguin-Landau-Verwey-Overbeek theory. Without or with very low amount of added phosphate, IOH particles have positive surface charge. In this first stage, both electrostatic interactions and van der Waals interactions further adhesion. The system is then in attractive coagulation statement, and the percentage of adhering bacteria is maximal. Following slight phosphate addition occurs the cancellation of IOH surface charge. Adhesion is then governed by the only van der Waals interactions, and the amount of adhering bacteria decrease to around 60% of the reference value (without phosphate). The addition of more phosphate reverses the surface charge of IOH, and the system behaves then in electrostatic repulsion. The electrostatic interactions would then stop adhesion in spite of van der Waals interactions. Bacterial adhesion is decreased to around 25% of the reference value but however still remains. This persisting adhesion may be attributed to the nature of bacterial surface, displaying large amounts of macromolecules allowing a "macro molecule bridging" with IOH and the occurrence of adhesion despite of electrostatic repulsion.

The negative surface charge of bacteria originates from the carboxyl groups which are the most common charged surface groups on the cell envelope of *E. coli SH 702* (Table 2). Thus, they are thought to be responsible for the interactions that take place in the first step of the attachment process of bacteria to the iron oxyhydroxide surface.

The role of carboxyl groups in the adsorption of organic matter on iron oxide surface was previously demonstrated by spectroscopy and modeling studies. It was shown that the complexation reactions between the carboxyl group and the surface of the iron oxide are responsible for the bonding of small weak organic acids to goethite (*5*, *38*, *43*). A similar reaction was demonstrated to be involved in the adsorption of natural organic matter onto iron oxide (*5*). These observations show that bacterial cells may be assimilated to macromolecules with large amounts of carboxyl surface groups responsible for bonding to the IOH surface.

The influence of phosphate on natural organic matter adsorption was observed by Geelhoed et al. (*34*). They compared the adsorption of phosphate and citrate in single anion systems or in competitive systems and showed that phosphate has a much larger intrinsic affinity for goethite than citrate. Phosphate anions were shown to reduce citrate adsorption onto goethite significantly. Thus, similar surface sites are involved in the adsorption of both carboxyl and phosphate anions onto goethite. This competition must be responsible for the limitation of bacterial adhesion in the presence of phosphate anions (Figure 4). IOH surface sites, preferentially bound to phosphate anions, can no longer bind to carboxyl.

Nevertheless, because of size incongruities, steric incompatibilities, and topographical and chemical heterogeneous surface of both particles, the adsorption of bacteria to minerals is unlikely to be strictly controlled by site-to-site interactions. The attachment of bacteria to IOH particles is not completely inhibited by phosphate, even when the particles are negatively charged (Figures 4 and 5). This proves that although electrostatic interactions are unfavorable to the adhesion process, other forces such as hydrophobicity, short-range acid−base interactions, steric interactions, and

van der Waals forces, sometimes described according to the extended-DLVO theory (*17*), still allow bacteria to adhere to the IOH surface. Moreover, the method used for the measurement of the surface charges gives only the resulting global charge of the surface. Residual positive surface sites may remain and allow bridging between particles. The literature demonstrates that even though surface charges are taken into account, hydrophobic interactions are mainly responsible for attachment (*17*, *44*−*46*), especially when both the bacterial and the solid surfaces are highly hydrophobic. Thus, correlations were preferentially made between the contact angle and/or hydrocarbon adhesion measures with attachment of bacteria to surfaces (*46*−*48*). When the contributions of the different forces involved in adhesion of bacteria to surfaces were compared, the electrostatic interactions became predominant, as the hydrophobicity of the systems was decreased (*49*). Surprisingly, positively charged IOH particles showed low adhesion to octane, which has highly negative zeta potential (*50*). This observation suggests that IOH would be hydrophilic. In such conditions, it becomes obvious that negatively charged phosphated IOH particles would not attach to octane, owing to hydrophobic and electrostatic repulsion (Table 1). In adhesion conditions (mineral water at pH 7), the (opposite) marked surface charges of both (phosphated-)IOH particles and bacterial cells are likely to make electrostatic interactions playing an important role in the adhesion process (Figure 5). At the same time, size measurements did not reveal any modifications in the volume of the particles (Table 1) as observed on amorphous hydroxide during phosphate adsorption (*51*), and because of the size of phosphate anions, no increase of steric interactions is to be expected. Therefore, the difference in the bacterial adhesion behavior with IOH and with phosphated IOH (Figure 4) is probably attributed to modifications of the surface charge, the occupation of surface sites by anions and to a lesser extent to the decrease in hydrophobicity.

This study demonstrated that the addition of phosphate is a mild way to limit bacterial adhesion to corrosion products efficiently. As the attachment process is thought to be a determinant stage in the colonization of the surface by bacteria (*16*), modifying the surface properties of the iron oxide may explain the decrease in bacterial activity observed during phosphate treatments on corroded pipes (*7*). The physicochemical properties of the surface then mediate the subsequent colonization behavior of the bacteria.

Acknowledgments

This work was carried out as part of a larger research program entitled “Biofilm VI” and coordinated by the Centre International de l’Eau de Nancy (NANCIE, France). It was funded by Agence de l’Eau Seine-Normandie (AESN, France), Anjou-Recherche (Générale des Eaux, France), Communauté Urbaine du Grand Nancy (CUGN, France), Office National de l’Eau Potable (ONEP, Morocco), Syndicat des Eaux d’Ile de France (SEDIF, France), and NANCIE. The authors thank J. Lambert (LCPME) for XPS analysis and J. Chevalier (Ecole Polythechnique de Montréal) for experimental help.

Literature Cited

(1) Emerson, D.; Weiss, J. V.; Megonigal, J. P. *Appl. Environ. Microbiol.* **1999**, *65*, 2758−2761.

(2) Little, B. J.; Ray, R. I.; Wagner, P. A.; Jones-Meehan, J.; Lee, C. C.; Mansfeld, F. *Biofouling* **1999**, *13*, 301−321.

(3) Roden, E.; Zachara J. M. *Environ. Sci. Technol.* **1996**, *30*, 1618−1628.

(4) Lovley, D. R. *Microbiol. Rev.* **1991**, *55*, 259−287.

(5) Gu, B.; Schmitt, J.; Chen, Z.; Liang, L.; McCarthy, J. F. *Environ. Sci. Technol.* **1994**, *28*, 38−46.

(6) Frateur, I.; Deslouis, C.; Kiéné, L.; Lévi, Y.; Tribollet, B. *Water Res.* **1999**, *33/8*, 1781−1790.

(7) Appenzeller, B. M. R.; Batté, M.; Mathieu, L.; Block, J. C.; Lahoussine, V.; Cavard, J.; Gatel, D. *Water Res.* **2001**, *35/4*, 1100−1105.

(8) Kerr, C. J.; Osborn, K. S.; Robson G. D.; Handley, P. S. *J. Appl. Microbiol. Symp. Suppl.* **1999**, *85*, 29s−38s.

(9) Donlan, R. M.; Pipes, W. O.; Yohe, T. L. *Water Res.* **1994**, *28*, 1497−1503.

(10) LeChevallier, M. W.; Lowry, C. D.; Lee, R. G.; Gibbon, D. L. *J. Am. Water Wks. Assoc.* **1993**, *85*, 59−71.

(11) Morin, P.; Gauthier, V.; Saby, S.; Block, J.-C. In *Biofilms in the aquatic environment*; Keevil et al., Eds., R.S.C.: Cambridge, 1999; pp 171−190.

(12) Herson, D. S.; McGonigle, B.; Payer, M. A.; Baker, K. H. *Appl. Environ. Microbiol.* **1987**, *53*, 1178−1180.

(13) Miettinen, I. T.; Vartiainen, T.; Martikainen, P. J. *Appl. Environm. Microbiol.* **1997**, *63/8*, 3242−3245.

(14) Sathasivan, A.; Ohgaki, S.; Yamamoto, K.; Kamiko, N. *Water Sci. Technol.* **1997**, *35/8*, 37−44.

(15) Schreppel, C. K.; Fredericksen, D. W.; Geiss, T. A. *WQTC. Denver, Nov.* **1997.**

(16) Busscher, H. J.; Bos, R.; Van der Mei, H. C. *FEMS Microbiol. Lett.* **1995**, *128*, 229−234.

(17) Ong, Y.-L.; Razatos, A.; Georgiou, G.; Sharma, M. M. *Langmuir* **1999**, *15*, 2719−2725.

(18) Achouak, W.; Thomas, F.; Heulin, T. *Colloids Surfaces B* **1994**, *3*, 131−137.

(19) Mafu, A. A.; Roy, D.; Goulet, J.; Savoie, L. *Appl. Environ. Microbiol.* **1991**, *57*, 1969−1973.

(20) Parfitt, R. L.; Atkinson, R. J. *Nature* **1976**, *264*, 740−741.

(21) Larsson, K.; Glantz, P.-O. *Acta Odontol. Scand.* **1981**, *39*, 79−82.

(22) Van der Mei, H. C.; De Vries, J.; Busscher, H. J. *Surf. Sci. Reports* **2000**, *39*, 1−24.

(23) *Standard Methods for the Examination of Water and Wastewater*, 20th ed.; American Public Health Association, American Water Works Association/Water Environment Federation: Washington DC, 1998.

(24) Rosenberg, M.; Gutnick, D.; Rosenberg, E. *FEMS Microbiol. Lett.* **1980**, *9*, 29−33.

(25) Fein, J. B.; Daughney, C. J.; Yee, N.; Davis, T. A. *Geochim. Cosmochim. Acta* **1997**, *61*, 3319−3328.

(26) Rijnaarts, H. H. M.; Norde, W.; Lyklema, J.; Zehnder, A. J. B. *Colloids Surf. B* **1995**, *4*, 191−197.

(27) Van der Mei, H. C.; Léonard, A. J.; Weerkamp, A. H.; Rouxhet, P. G.; Busscher, H. J. *Colloids Surf.* **1988**, *32*, 297−305.

(28) Van der Wal, A.; Norde, W.; Zehnder A. J. B.; Lyklema, J. *Colloids Surf. B* **1997**, *9*, 81−100.

(29) Li, J.; McLandsborough L. A. *Intl. J. Food Microbiol.* **1999**, *53*, 185−193.

(30) Amro, N. A.; Kotra, L. P.; Wadu-Mesthrige, K.; Bulychev, A.; Mobashery, S.; Liu, G. *Langmuir* **2000**, *16*, 2789−2796.

(31) Sleytr, U. B.; Messner, P.; Minnikin, D. E.; Heckels, J. E.; Virji, M.; Russell, R. B. B. In *Bacterial cell surface techniques*; Hancock, I. C., Poxton, I. R., Eds.; John Wiley & Sons: New York, 1988.

(32) Beech, I. B.; Edyvean, R. G. J.; Cheung, C. W. S.; Turner, A. *European Federation of Corrosion Publications*; Number 15, Microbial Corrosion, Proc. of the 3rd Int. EFC Workshop, Portugal, 1994; pp 329−337.

(33) Bowden, J. W.; Nagarajah, S.; Barrow, N. J.; Posner, A. M.; Quirk, J. P. *Aust. J. Soil Res.* **1980**, *18*, 49−60.

(34) Geelhoed, J. S.; Hiemstra, T.; Van Riemsdijk, W. H. *Environ. Sci. Technol.* **1998**, *32*, 2119−2123.

(35) Barrow, N. J.; Brümmer, G. W.; Strauss, R. *Langmuir* **1993**, *9*, 2606−2611.

(36) Torrent, J.; Barron, V.; Schwertmann, U. *Soil Sci. Soc. Am. J.* **1990**, *54*, 1007−1012.

(37) Ioannou A., Dimirkou A.; Papadopoulos P. *Commun. Soil. Sci. Plant. Anal.* **1998**, *29*(11−14), 2175−2190.

(38) Hiemstra T.; Van Riemsdijk W. H. *J. Coll. Int. Sci.* **1996**, *179*, 488−508.

(39) Ognalaga, M.; Frossard, E.; Thomas, F. *Soil Sci. Soc. Am. J.* **1994**, *58*, 332−337.

(40) Solari, J. A.; Huerta, G.; Escobar, B.; Vargas, T.; Badilla-Ohlbaum, R.; Rubio, J. *Colloids Surf.* **1992**, *69*, 159−166.

(41) Harkes, G.; Feijen, J.; Dankert, J. *Biomaterials* **1991**, *12*, 853−859.

(42) Yee, N.; Fein, J. B.; Daughney, C. J. *Geochim. Cosmochim. Acta* **2000**, *64*, 609−617.

(43) Filius, J. D.; Hiemstra, T.; Van Riemsdijk, W. H. *J. Colloid Interface Sci.* **1997**, *195*, 368−380.
(44) Ohmura, N.; Kitamura, K.; Saiki, H. *Appl. Environ. Microbiol.* **1993**, *59/12*, 4044−4050.
(45) Burchard, R. P.; Rittschof, D.; Bonaventura, J. *Appl. Environm. Microbiol.* **1990**, *56/8*, 2529−2534.
(46) Stenström, T. A. *Appl. Environ. Microbiol.* **1989**, *55/1*, 142−147.
(47) Caccavo, F. JR.; Schamberger, P. C.; Keiding, K.; Nielsen, P. H. *Appl. Environ. Microbiol.* **1997**, *63/10*, 3837−3843.
(48) Bendinger B.; Rijnaarts, H. H. M.; Altendorf, K.; Zehnder, A. J. B. *Appl. Environ. Microbiol.* **1993**, *59/11*, 3973−3977.
(49) Van Loosdrecht, M. C. M.; Lyklema, J.; Norde, W.; Schraa, G.; Zehnder, A. J. B. *Appl. Environ. Microbiol.* **1987**, *53/8*, 1898−1901.
(50) Van der Mei, H. C.; Van de Belt-Gritter, B.; Busscher, H. J. *Colloids Surf. B: Biointerfaces* **1995**, *5*, 117−126.
(51) Yamaguchi, N.; Hashitani, T.; Okazaki, M.; Takeda, T. *J. Colloid Interface Sci.* **1996**, *183*, 280−284.

Received for review May 30, 2001. Revised manuscript received October 18, 2001. Accepted November 2, 2001.

ES010155M